PNAS
www.pnas.org

Supplementary Information for

Circadian misalignment induces fatty acid metabolism gene profiles and compromises insulin sensitivity in human skeletal muscle

Jakob Wefers, Dirk van Moorsel, Jan Hansen, Niels Connell, Bas Havekes, Joris Hoeks, Wouter van Marken Lichtenbelt, Hélène Duez, Esther Phielix, Andries Kalsbeek, Mark V. Boekschoten, Guido J. Hooiveld, Matthijs K.C. Hesselink, Sander Kersten, Bart Staels, Frank A.J.L. Scheer, Patrick Schrauwen

Prof. Patrick Schrauwen, PhD
Email: p.schrauwen@maastrichtuniversity.nl

This PDF file includes:

Supplementary text
Figs. S1 to S6
References for SI reference citations

www.pnas.org/cgi/doi/10.1073/pnas.1722295115

Supplementary Information Text

Materials and Methods

Pre-study conditions. Three days before the study periods, participants were instructed not to perform physical exercise. Two days before each in-laboratory study protocol, participants were provided with meals to ensure standardized distribution of calories and macronutrients (see below). Compliance to the prescribed lifestyle was monitored with food- and sleep diaries and by a light-detecting wrist accelerometer (Actiwatch Spectrum, Philips-Respironics, Murrysville PA, USA).

Study conditions. The screen emittance of the TV and computer in the respiration chamber were adapted to not exceed the permitted light intensity of 4 lux and could be used to work, listen to music or watch movies. During their stay, participants were isolated from external time cues and only were in contact with the researchers. For specific study procedures (placement of intravenous cannula, indirect calorimetry, skeletal muscle biopsy, and the hyperinsulinemic euglycemic clamp), participants were transported to an adjacent clinical room in a wheelchair, during which they wore a blindfold and earplugs to prevent excess light and possible audiovisual cues that might indicate whether it was day or night. The clinical room had similar dim-light conditions as the respiration chamber. During procedures for which light was required (placement of intravenous canula or muscle biopsy), participants wore welding goggles shade 5 (Uvex Ultravision 9301-245, Uvex, Fürth, Germany) to limit light exposure.

Study design. Participants were instructed to follow a standardized lifestyle with fixed activities at fixed time points (making the bed, doing the dishes, 15-minutes standing, sitting at desk, or free time) to prevent differences between the 2 study conditions. Sleeping metabolic rate was measured by whole-room indirect calorimetry (Omnical, Maastricht Instruments, Maastricht, The Netherlands) during the first night, which was used for estimation of caloric requirements.

After waking up on the third study day, participants ingested a thermometer capsule (Equivital, Philips-Respironics, Murrysville PA, USA) to measure core-body temperature (CBT) for 24 hours. Due to early excretion of the capsule or technical failure, complete CBT measurements were obtained in 8 participants only. At 7 PM on day 3, participants underwent a blood draw, directly followed by a 30-minute resting indirect calorimetry measurement and a skeletal muscle biopsy (see below). During the sleep opportunity between day 3 and 4, we measured sleeping metabolic rate in the respiration chamber by whole-room indirect calorimetry (Omnical, Maastricht Instruments, Maastricht, The Netherlands). Activity levels during scheduled sleep were measured by a custom built analog ultrasound system (IDEE Maastricht University, Maastricht, The Netherlands) with continuous movement detection which is sampled and converted to a digital signal at 60 Hz. Data were averaged over a time span of 5 minutes. The implementation of the radar system has been described before (1).

On the fourth study day, participants were woken up at 6:45 AM. Starting at 7 AM, an intravenous cannula was placed in the antecubital vein, followed by a blood draw, indirect calorimetry and skeletal muscle biopsy, similar to the previous day. After the biopsy, a two-step hyperinsulinemic euglycemic clamp was performed to assess insulin sensitivity (see below). During this test, participants remained fasted. Directly after the clamp (which takes approximately 8 hours), participants were provided with a meal and were allowed to go home as soon as plasma glucose was stabilized.

In the misaligned period, breakfast, lunch, snack and dinner were served at 8 PM, 12:30 AM, 3 AM and 8 AM and consecutive sleep opportunities were scheduled from 11 AM until 7 PM. Blood drawing, indirect calorimetry and skeletal muscle biopsies were performed on day 4 at 7 AM (behavioral evening) and at 7 PM (behavioral morning). The two-step hyperinsulinemic euglycemic clamp started after the 7 PM biopsy.

Study meals. Standardized meals for two days before and during the study were prepared according to Dutch dietary guidelines (2). Caloric requirements for consumption at home and the first evening of the study period were calculated by multiplying the resting metabolic rate, estimated using the Harris-Benedict formula (3), with an activity factor of 1.5. In addition, as it is difficult to predict the exact energy expenditure of the participants, additional snacks were provided to reach an energy intake equal to the resting metabolic rate multiplied by a factor of 1.7. Participants were allowed to eat these additional snacks directly after their meals, only if they were still hungry.

Indirect calorimetry. Calculations of energy expenditure and substrate oxidation were made with the assumption of a negligible protein oxidation (4, 5).

Two-step hyperinsulinemic euglycemic clamp. A primed-continuous infusion of D-[6,6-$^{2}H_{2}$]glucose was given for two hours to determine baseline endogenous glucose production (EGP), glucose appearance (Ra) and glucose disposal (Rd) (6). Blood was frequently sampled and glucose levels directly analyzed in arterialized blood. Glucose was co-infused at an appropriate rate to maintain euglycemia (~5.0 mmol/L). During the last 30 minutes of each step, substrate oxidation was measured by indirect calorimetry.

High resolution respirometry. For the 7 AM and 7 PM (pre-clamp) biopsies, part of the biopsy was immediately placed in ice-cold preservation medium (BIOPS, OROBOROS Instruments, Innsbruck, Austria) and used for measurement of mitochondrial oxygen consumption. For this analysis, intact muscle fibers were permeabilized and oxygen consumption rate was measured upon several substrates using high-resolution respirometry (Oxygraph, OROBOROS Instruments, Innsbruck, Austria). Substrates used to consecutively supplement muscle fibers during this assay were octanoylcarnitine (trace 1) or pyruvate (trace 2), as described previously (7). Uncoupled respiration was assed using carbonylcyanide p-trifluoromethoxyphenylhydrazone (FCCP). The remaining part of the muscle biopsy was immediately frozen in melting isopentane and stored at -80°C until further analysis.

Structural components of the mitochondrial electron transport chain complexes were quantified by western blot analysis as previously described (8). Briefly, human muscle tissue was lysed in RIPA buffer and protein concentration was determined using the Bio-Rad RC/DC kit (Bio-Rad Laboratories, Veenendaal, The Netherlands). Equal amounts of protein were loaded on 12% TGX gels (Bio-Rad Laboratories) and proteins were transferred to nitrocellulose with the Trans-Blot Turbo transfer system (Bio-Rad Laboratories). Primary antibodies: a cocktail of mouse monoclonal antibodies directed against human OXPHOS (dilution 1:10,000; ab110411, Abcam, Cambridge, UK). The specific proteins were detected using secondary antibodies conjugated with IRDye800, and were quantified with the CLx Odyssey Near Infrared Imager (Li-COR, Westburg, Leusden, The Netherlands). The individual total intensity of Complex I, II, III, IV and V was quantified and is expressed in arbitrary units (AU).

Gene transcript quantification. To minimize the variability in reference gene normalization, the geometric mean of three reference genes (RPL26, GUSB and CYPB) was used, which were previously demonstrated to be expressed robustly independent of time (8, 9). This geometric mean served as the internal reference for comparative gene expression analysis in the remainder of the study.

Microarray processing and data analysis. RNA quality was assessed using RNA 6000 nanochips on the Agilent 2100 bioanalyzer (Agilent Technologies, Amstelveen, the Netherlands). Sample labelling, hybridization to chips and image scanning was performed according manufacturer's instructions. Quality control and data analysis pipeline have been described in detail previously (10). Briefly, normalized expression estimates of probe sets were computed by the robust multiarray analysis (RMA) algorithm (11) as implemented in the Bioconductor package *affyPLM*. Probe sets were redefined using current genome information according to Dai *et al.* (12) based on annotations provided by the Entrez Gene database, which resulted in the profiling of 29,526 unique genes (custom CDF v22). To evaluate whether samples could be separated based on their gene expression profiles, multilevel partial least squares-discriminant analysis (PLS-DA) was performed, as implemented in the package *mixOmics* (13). Differentially expressed probe sets (genes) were identified by using linear models (package *limma*) and an intensity-based moderated paired t-statistic (14, 15). By blocking on subject in the design matrix the crossover design of the study was taken into account. P-values were corrected for multiple testing by a false discovery rate (FDR) method (16). Changes in gene expression were related to changes in pathways by gene set enrichment analysis (GSEA) (17) using the Bioconductor package *fgsea* (18) and the subset of metabolic and signalling pathways retrieved from the expert-curated Kyoto Encyclopedia of Genes and Genomes (KEGG) database (19). Only gene sets consisting of more than 10 and fewer than 500 genes were taken into account, which resulted in the inclusion of 226 gene sets. A list of human PPAR targets genes was obtained from (20). For each comparison, genes were ranked on their absolute t-value that was calculated by the empirical Bayes method (21). Statistical significance of GSEA results was determined using 10,000 permutations. Results were visualized using the Bioconductor package *clusterProfiler* (22). Microarray data have been submitted to the Gene Expression Omnibus GSE106800.

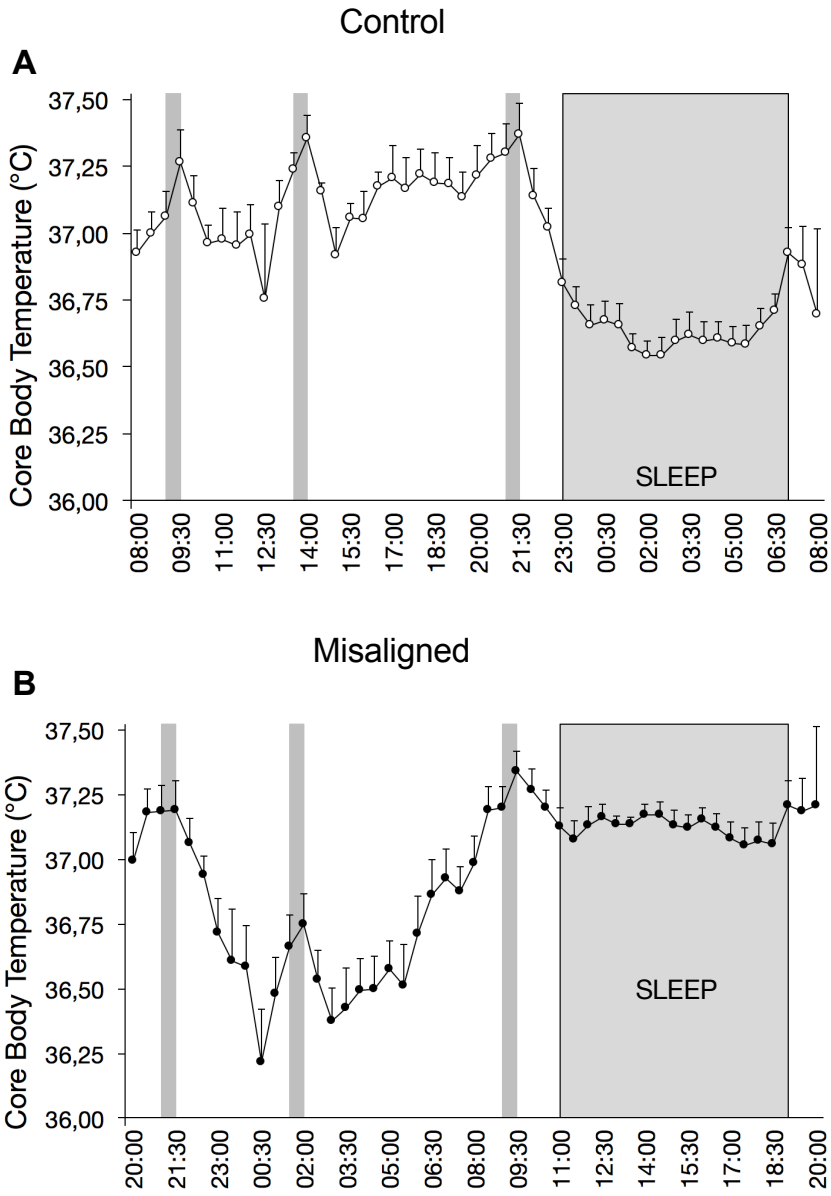

Fig. S1. Core Body Temperature (CBT) in the control and misalignment condition. Core body temperature (°C) recordings were obtained every 15 seconds and averaged per subject into 30 min intervals. Depicted are the control condition (A) and misalignment condition (B). Sleeping periods are indicated by wide grey bars. The small grey bars indicate 30-min bouts of physical activity performed one hour after each meal. Data is expressed as mean ± SEM of 8 subjects. * $p < 0.05$.

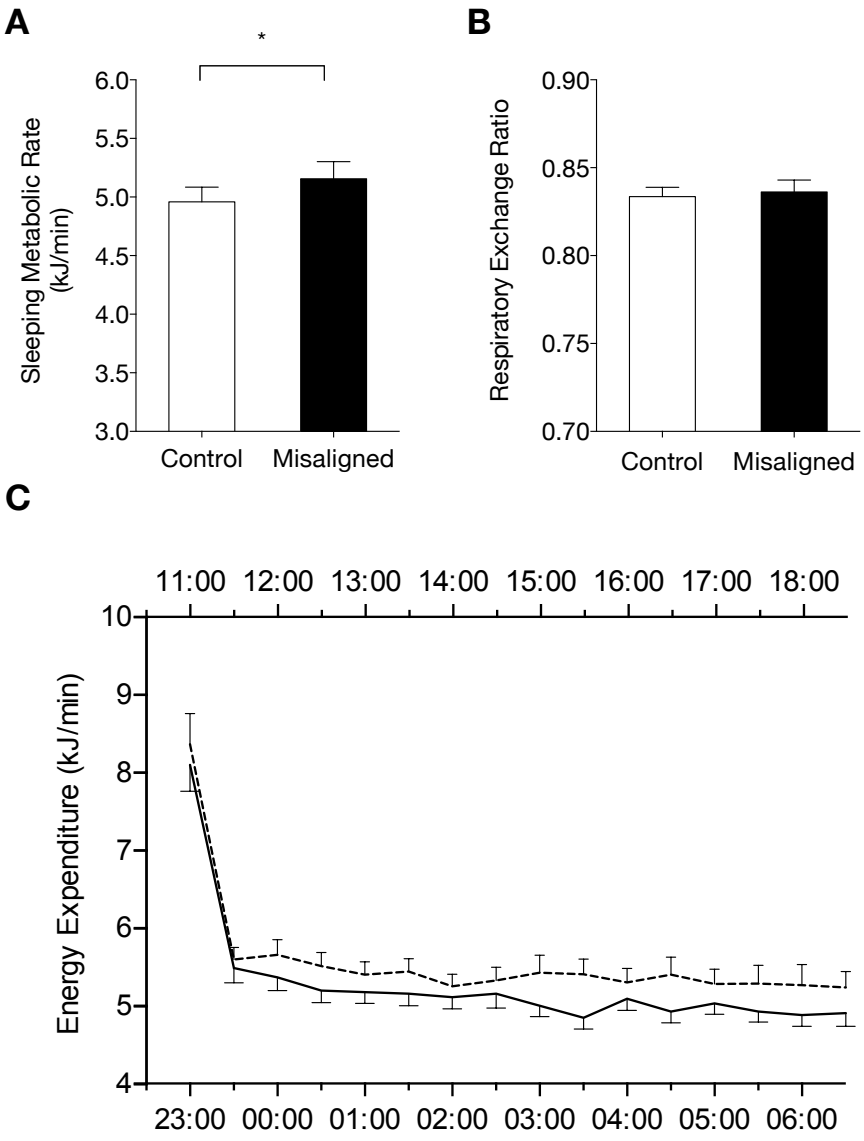

Fig. S2. Sleeping Metabolic Rate (SMR) is increased in circadian misalignment. Sleeping metabolic rate was measured in a whole-body room calorimeter and defined as the lowest energy expenditure during scheduled sleep during three consecutive hours (A). Respiratory Exchange Ratio (RER) during the same period is depicted in (B). As can be seen in (C), the increased metabolic rate during circadian misalignment was present during the entire sleeping period. Time is displayed as clock hours (misaligned time on upper axis). Data is expressed as mean ± SEM. * $p < 0.05$.

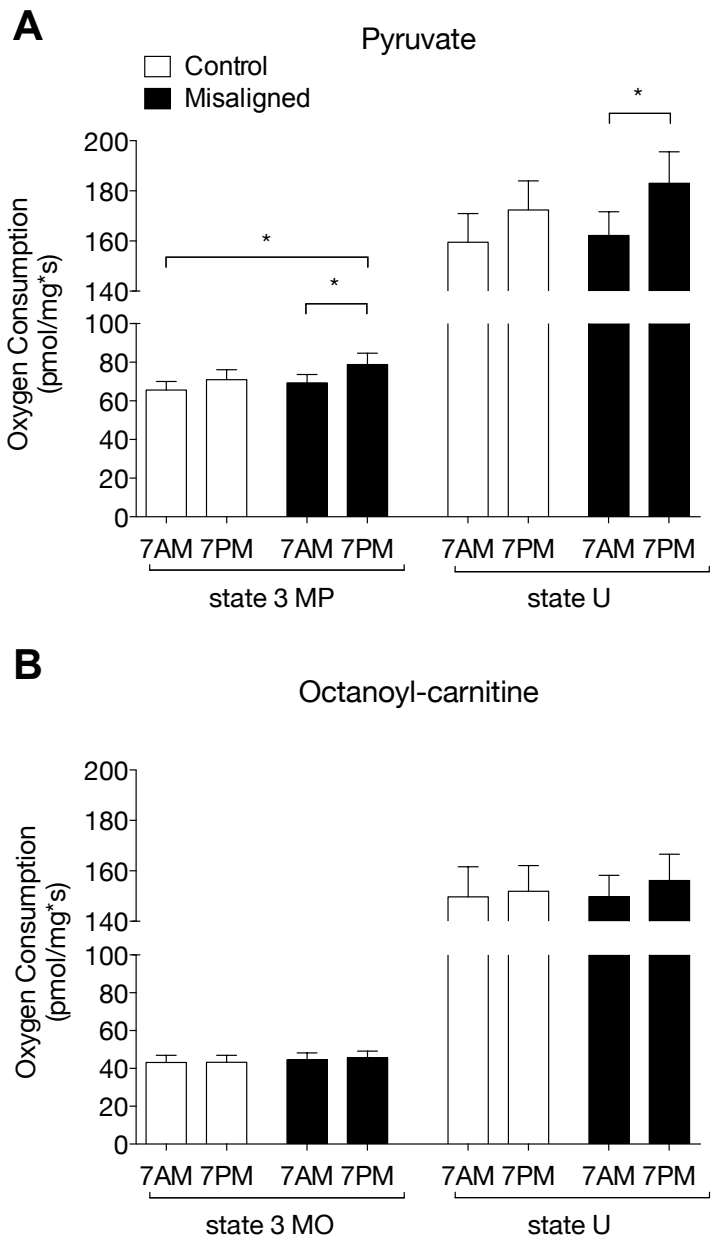

Fig. S3. Mitochondrial oxidative capacity in the behavioral morning and evening. ADP stimulated mitochondrial respiration (state 3) and maximal uncoupled (state U) respiration in isolated permeabilized muscle fibers upon pyruvate (A) or octanoylcarnitine (B) as a substrate. M, malate; O, octanoylcarnitine; P, pyruvate. Data represents oxygen consumption rates per mg wet weight per second, depicted as mean ± SEM. * $p < 0.05$.

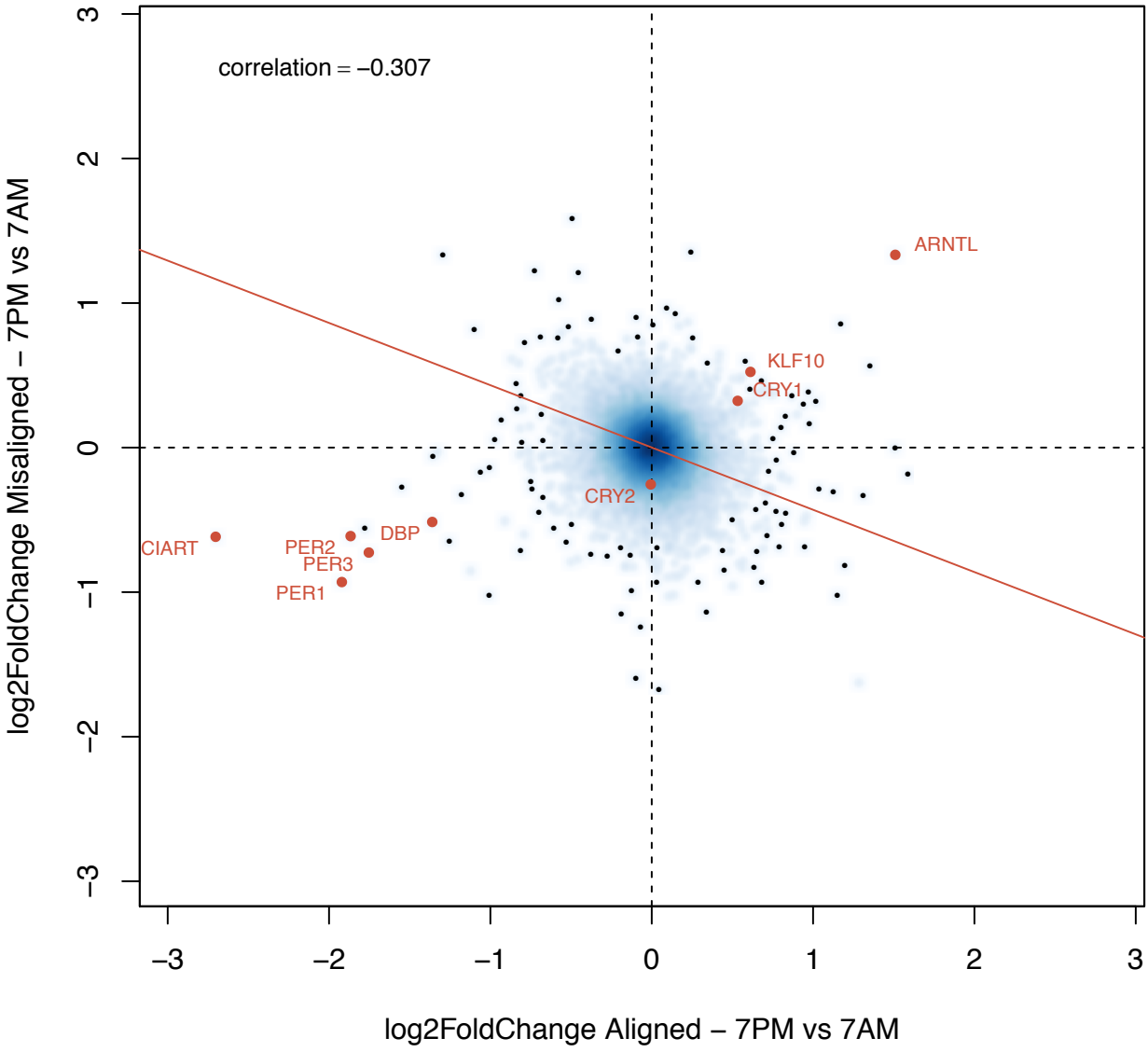

Fig. S4. Differences in gene expression patterns (7 AM vs. 7 PM) between study conditions of individual genes. Depicted is a scatterplot based on log (base 2) fold changes (group mean) between the timepoints 7 AM (reference time point) and 7 PM in the control and misaligned condition. Correlation line indicates that the majority of genes tend to have a reversed expression pattern in the misaligned condition, suggesting they only partly align to behavioral rhythm. Genes that are clock related and that are known to display a circadian rhythm are highlighted in red. These genes tend to align into an opposite direction compared to the regression line suggesting they do not align to behavioral rhythm.

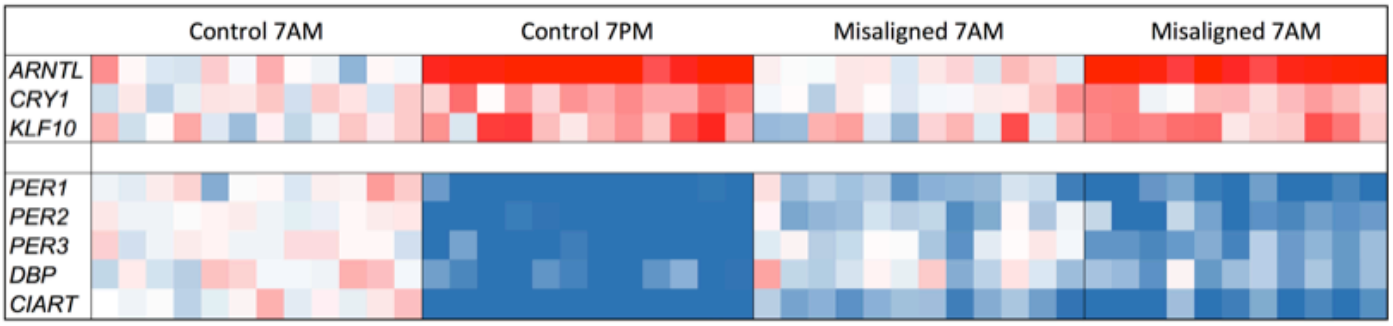

Fig. S5. Circadian clock genes of individual subjects show consistent differences in expression levels between 7 AM and 7 PM. Heatmaps showing inter-individual differences in gene expression using 7 AM in the control condition as a reference. Red color indicates higher expression and blue color indicates lower expression. Differences are based on log (base 2) fold changes with the group mean expression level at 7 AM in the control condition set at 0.

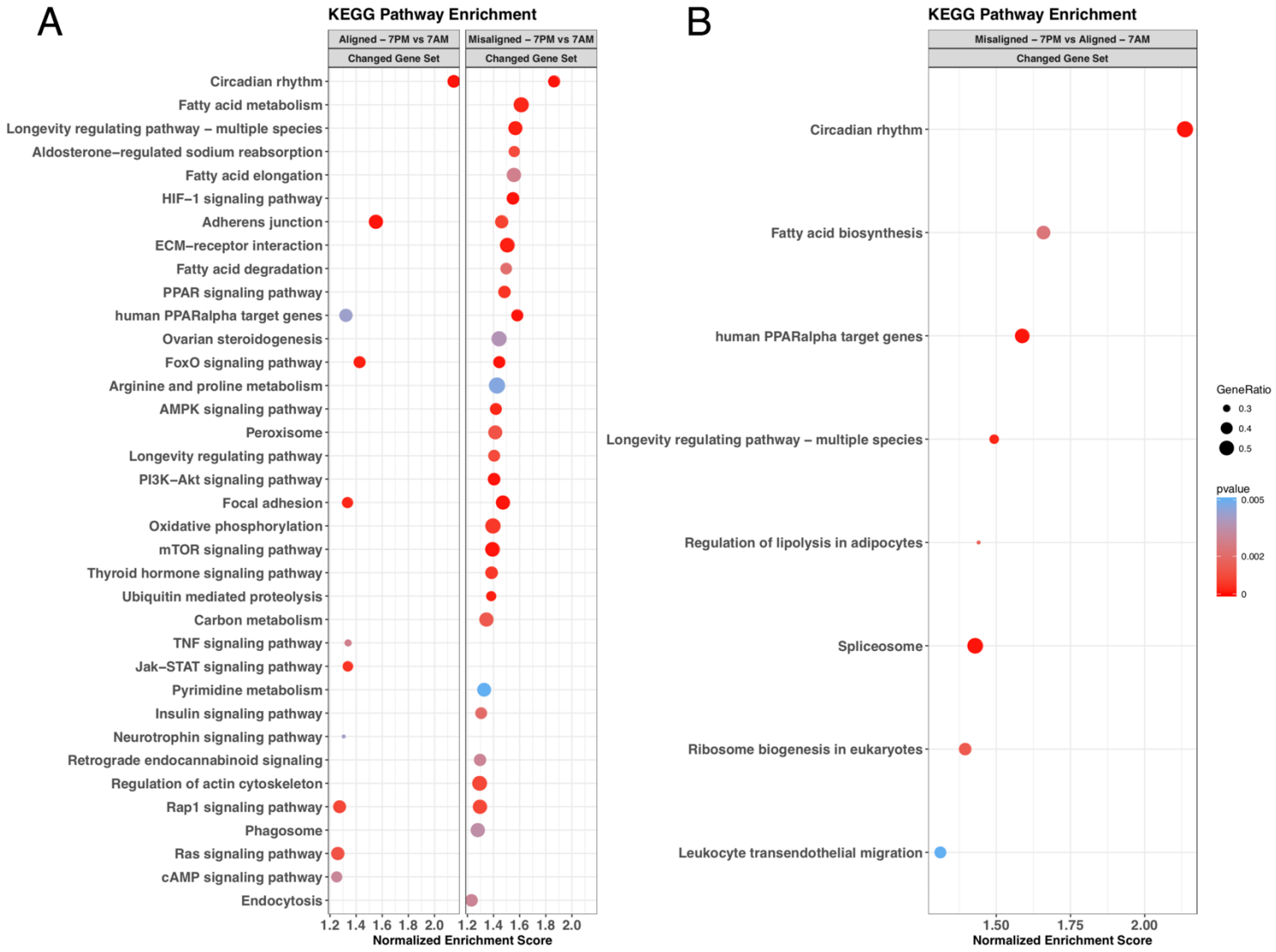

Fig. S6. Regulation of fatty acid metabolism and PPAR signaling at the 7 PM misaligned condition. (A) Changes in gene expression of individual genes (group mean) from 7 AM (reference timepoint) to 7 PM in the control and misaligned condition were used to determine the change in pathway activity. Directionality of change in pathway activity (either activated or inhibited) is not taken into account. Pathways are ranked according to the normalized enrichment score (NES). A high NES score indicates changed activity of the pathway at 7 PM compared to 7 AM in either the control or misaligned condition. Pathway analysis was performed on the basis of the 226 metabolic and signaling pathway subset from the KEGG database. (B) Changes in gene expression of individual genes (group mean) from 7 AM in the control condition to 7 PM in the misaligned condition were used to determine the change in pathway activity by GSEA. A high NES score indicates changed activity of the pathway at 7 PM compared to 7 AM in either the control or misaligned condition. Pathway analysis was performed on the basis of the 226 metabolic and signaling pathway subset KEGG database.

References

1. Schoffelen PF, Westerterp KR, Saris WH, & Ten Hoor F (1997) A dual-respiration chamber system with automated calibration. *J Appl Physiol (1985)* 83(6):2064-2072.
2. Kromhout D, Spaaij CJ, de Goede J, & Weggemans RM (2016) The 2015 Dutch food-based dietary guidelines. *Eur J Clin Nutr* 70(8):869-878.
3. Harris JA & Benedict FG (1918) A Biometric Study of Human Basal Metabolism. *Proc Natl Acad Sci U S A* 4(12):370-373.
4. Peronnet F & Massicotte D (1991) Table of nonprotein respiratory quotient: an update. *Can J Sport Sci* 16(1):23-29.
5. Weir JB (1949) New methods for calculating metabolic rate with special reference to protein metabolism. *J Physiol* 109(1-2):1-9.
6. Mensink M, Blaak EE, van Baak MA, Wagenmakers AJ, & Saris WH (2001) Plasma free Fatty Acid uptake and oxidation are already diminished in subjects at high risk for developing type 2 diabetes. *Diabetes* 50(11):2548-2554.
7. Hoeks J*, et al.* (2010) Prolonged fasting identifies skeletal muscle mitochondrial dysfunction as consequence rather than cause of human insulin resistance. *Diabetes* 59(9):2117-2125.
8. van Moorsel D*, et al.* (2016) Demonstration of a day-night rhythm in human skeletal muscle oxidative capacity. *Mol Metab* 5(8):635-645.
9. Hansen J*, et al.* (2016) Synchronized human skeletal myotubes of lean, obese and type 2 diabetic patients maintain circadian oscillation of clock genes. *Sci Rep* 6:35047.
10. Lin K*, et al.* (2011) MADMAX - Management and analysis database for multiple ~omics experiments. *J Integr Bioinform* 8(2):160.
11. Irizarry RA*, et al.* (2003) Exploration, normalization, and summaries of high density oligonucleotide array probe level data. *Biostatistics* 4(2):249-264.
12. Dai M*, et al.* (2005) Evolving gene/transcript definitions significantly alter the interpretation of GeneChip data. *Nucleic Acids Res* 33(20):e175.
13. Rohart F, Gautier B, Singh A, & Le Cao KA (2017) mixOmics: An R package for 'omics feature selection and multiple data integration. *PLoS Comput Biol* 13(11):e1005752.
14. Sartor MA*, et al.* (2006) Intensity-based hierarchical Bayes method improves testing for differentially expressed genes in microarray experiments. *BMC Bioinformatics* 7:538.
15. Ritchie ME*, et al.* (2015) limma powers differential expression analyses for RNA-sequencing and microarray studies. *Nucleic Acids Res* 43(7):e47.
16. Benjamini Y & Hochberg Y (1995) Controlling the False Discovery Rate: A Practical and Powerful Approach to Multiple Testing. *Journal of the Royal Statistical Society. Series B (Methodological)* 57(1):289-300.
17. Subramanian A*, et al.* (2005) Gene set enrichment analysis: a knowledge-based approach for interpreting genome-wide expression profiles. *Proc Natl Acad Sci U S A* 102(43):15545-15550.
18. Sergushichev A (2016) An algorithm for fast preranked gene set enrichment analysis using cumulative statistic calculation. *bioRxiv*.
19. Kanehisa M, Sato Y, Kawashima M, Furumichi M, & Tanabe M (2016) KEGG as a reference resource for gene and protein annotation. *Nucleic Acids Res* 44(D1):D457-462.
20. Rakhshandehroo M, Knoch B, Muller M, & Kersten S (2010) Peroxisome proliferator-activated receptor alpha target genes. *PPAR Res* 2010.
21. Nam D (2017) Effect of the absolute statistic on gene-sampling gene-set analysis methods. *Stat Methods Med Res* 26(3):1248-1260.
22. Yu G, Wang LG, Han Y, & He QY (2012) clusterProfiler: an R package for comparing biological themes among gene clusters. *OMICS* 16(5):284-287.